



THE SEASONAL EFFECT ON THE WATER BODIES IN IRAQI MARSHLANDS

Taghreed A.H. Naji and Hameed M. Abduljabbar

^a Department of Physics, College of Education for Pure Science Ibn-Al-Haitham, University, of Baghdad, Baghdad, Iraq.

Abstract

In this research, the seasonal effect on the water bodies of the Iraqi marshlands are monitored by calculating the areas and percentages for the period 1987 to 2017 of the Summer and Winter seasons using Support Vector Machine (SVM) classifier, where the differences between the two seasons are calculated and an empirical equation is implemented for it. Comparison for three different water bodies classes (shallow, deep and very deep) between the Summer and Winter seasons are presented.

The results showed the recovery of Iraq's marshlands in the Winter season more than the Summer, Beside that the differences between the water bodies for the Summer and Winter seasons for the late 30 years are encounter a continues reduction due to the reduction in the water levels, which gave a clear and comprehensive picture of the change of water type with the two seasons.

Key words: Iraqi marshland, land cover, Landsat images, Digital analysis, Temporal change detection, Support Vector Machine (SVM) classification.

Introduction

The Iraq marshlands region is chosen, due to its economic and ecological importance. It is a unique aquatic environment in Iraq that differs from other aquatic environments (AL-Ghafily, 2009). Marshlands are small lakes and ponds full. They are continually flooded wetland, not useless regions as they have often been understood, but they are among the most productive region in the world (Saleh and Nasser, 2014). These specific wetlands are at the southern part of Iraq, progress a vital part in the conservation of biodiversity in the Middle East. Because of their large size, the richness of their aquatic vegetation and their segregation from other similar systems (Bedair *et al.*, 2006). Wetlands are a natural sponge when floodwaters overflow the banks of streams wetland soak up an enormous amount of the surplus water, then infiltrates slowly back into the stream to prevent downstream flooding. In drought times, wetlands are fed by groundwater which is sent out into streams to store them streaming year-round (Saleh & Nasser, 2014).

The Marshlands environment is a reserve for many

natural plants, wild animals. Until the 1970s, the marshland covered an area of approximately 15,000 km² around the southern part of the Tigris and Euphrates rivers, but they were reduced after drying to about 10 percent of their area (Anon., n.d.). It has been subjected to exceptional circumstances in which various political and economic factors have been intertwined, as well as other variables that have taken place in Iraq and its vicinity. Security and military measures have affected the environment of the region by diverting rivers and dams and thus drying them (Anon., n.d.) (Albarakat *et al.*, 2018). Monitoring water regions change is very important to gain the best scientific understanding of the recovery process and to aiding decision-makers to plan and implement appropriate repair (Jaquet *et al.*, 2005). Temporal change detection is a very important process that helps in determining the changes of water bodies over large areas and for long period, with continuation monitoring using multi-temporal remote sensing data capabilities (Muhsin and Kadhim, 2017) (Saleh, 2012). Hence, we need to conduct this research to follow up and study the seasonal changes of the Marshlands of Iraq.

***Author for correspondence** : E-mail: taghreednaji1972@gmail.com, hameed.m.aj@ihcoedu.uobaghdad.edu.iq

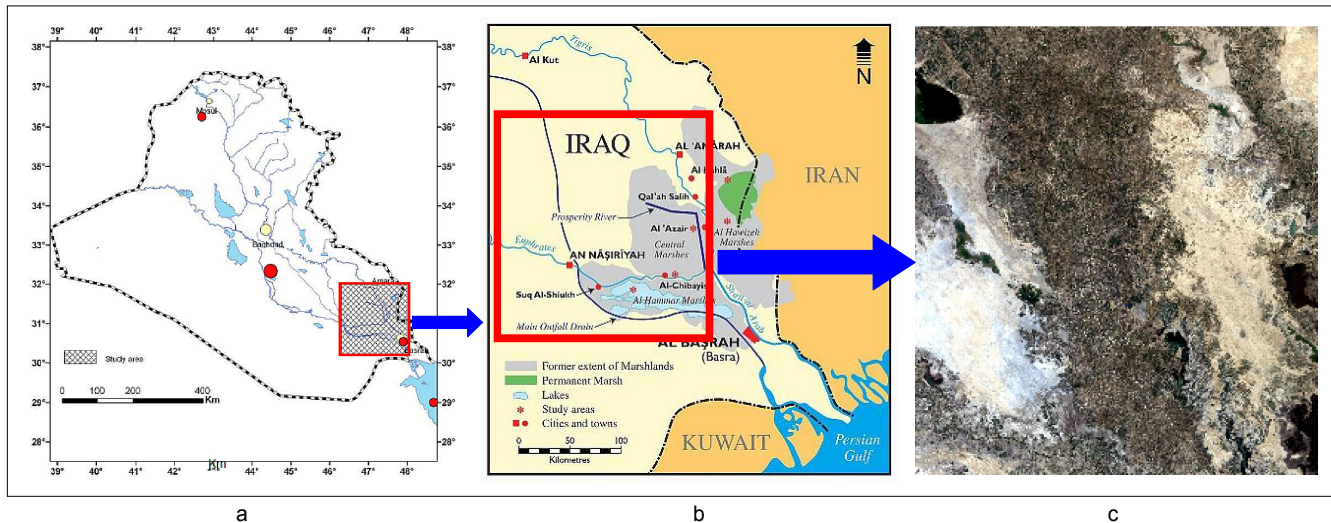


Fig. 1: a. location map of Iraq (Abdul Jabbar, *et al.*, 2010), b. A map representing the Iraq marshes region (Fitzpatrick, 2004) and c. True color of (Landsat-5 TM) study scene.

Satellite remotely sensed imagery is the only tool to demonstrate the changes taking place on a continuous (Jaquet *et al.*, 2005). It can be made use in the evaluation of environmental damage by computing the seasonal changes for water bodies to support the sustainable management of Iraq marshlands by monitoring water regions to provide objective and up to date information and to disseminate devices needed for assessment and management (Abed Al-Razaq *et al.*, 2015). The facilities which are presented by the remote sensing technique, such as, fast, cost, time, effort and comprehensive vision

Table 1: The support vector machine classification parameters.

Gamma in Kernel Function	Penalty Parameter	Pyramid Levels	Classification Probability Threshold
0.1	100	0	0

Table 2: The Adopted Landsat scenes for Summer and Winter seasons and their corresponding classification accuracy.

No.	Date	Satellite	Accuracy %
1.	17 January 1987	Landsat_5 TM	98.6606
2.	12 July 1987	Landsat_5 TM	100.0000
3.	11 December 1990	Landsat_5 TM	98.8427
4.	4 July 1990	Landsat_5 TM	99.4819
5.	23 January 1995	Landsat_5 TM	98.2019
6.	18 July 1995	Landsat_5 TM	98.9772
7.	6 February 2000	Landsat_5 TM	99.0502
8.	31 July 2000	Landsat_5 TM	98.6867
9.	11 June 2005	Landsat_5 TM	99.8952
10.	24 January 2007	Landsat_5 TM	97.7998
11.	12 February 2014	Landsat_8 OLI	99.4824
12.	22 July 2014	Landsat_8 OLI	98.6009
13.	4 February 2017	Landsat_8 OLI	98.9415
14.	12 June 2017	Landsat_8 OLI	98.4820

to separate the objects of a certain region on the other regions detect the ability to use this technique for water and other objects (Muhsin, 2011).

Iraq marshlands occupied the wide scope of researches such as, in Abdul Jabbar and *et al.*, 2010, detect the changes in land use and land cover using changes detection method by remote sensing techniques for Landsat images: MSS in 1973, TM in 1990 and ETM+ in 2000. The percentage area of each class is determined from the total coverage of marshland regions. They show the large changes were between 1973 and 2000 in land cover and land use. The dry land is increased and the water bodies are decreased, with desertification is increased causing big environmental and hydrological changes that influenced the physical and chemical properties of the soil. The soil became not suitable for agricultural procedures. In Israa, 2011 (Muhsin, 2011), monitors the main changes by satellite images acquired of Landsat MSS 1973, TM 1990, 2002 and MODIS 2010 marshland. The scene of Landsat MSS 1973 marshland consider to be stable and environmental equilibrium case, hence it represented a reference scene for the marshlands region. The classification result of Landsat TM 1990 marshland showed the water bodies extension in the Al-Hawizeh marshland with decreasing of the vegetation cover in the eastern part of the marsh. The Water class was occupying Al-Murays and Umm Al-Naaj lakes in Landsat ETM+2002 result. Landsat MSS, 2010 classification result illustrated a restoration for the marshlands region by its inundation with water, after removal of the barriers and opening the outlets that supply the water from Al-Musharah and Al-Kahlaa rivers into the eastern part from Tigris River. Muhsin and Kadhim, 2017 showed the deep-water region increases 1242.55

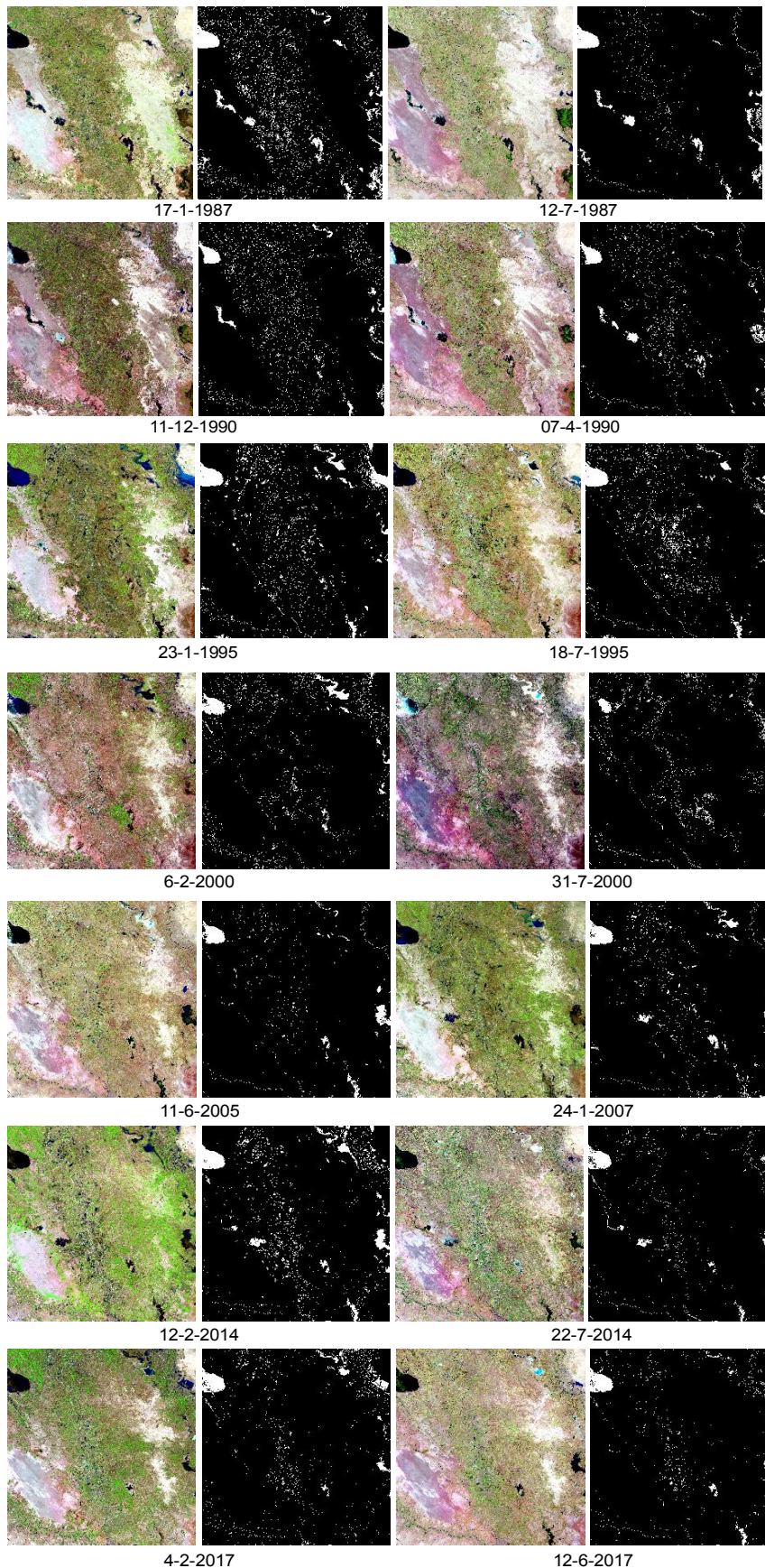


Fig. 2: Pseudo band combination of the Landsat scenes and extracted water bodies using SVM classification method.

km² from the period 1973 to 2014 for south Iraq marshes. While the shallow water region decreases 823.17 km² in Iraq marshland 2014 compared with 1984.

Support Vector Machine (SVM) supervised classifier is used in this research work to distinguish between the different land cover types in the marshlands area, many researcher used this classifier in classification of the marshlands (Ma and Guo, 2014) (Suykens *et al.*, 2015) (Salman, 2019) (Naji and Hatem, 2013).

Seasonal variation of overall water bodies and its classes were obtained by calculating the difference and change detection method, using ENVI 5.3 program. The change of water regions was monitored within the period between 1987 to 2017.

Temporal change detection is very important process that helps in determining the changes of water bodies over large areas and for long period, with continuation monitoring using multi temporal remote sensing data capabilities.

To fulfill this study, Landsat (TM 1987, 1990, 1995, 2000, 2005, 2007 and OLI 2014, 2017) for Iraqi marshland region are used.

Materials and Methods

Study area description

Iraqi marshlands consist of a big triangular region bounded by three main southern cities, Nasiriyah to the west, Amarah to the northeast, and Basrah to the south (Fig. 1b). They include both permanent and seasonal marshlands. Three important regions are the Al-Hammar (3.5×10^6) Km², the Central (such as, Al-Shuweijahh, dlameg, Ibn Najm, Saadia, Ouda, Sunni and Al-Chabaish marshes) (3×10^6) Km² and Al-Hawizeh and its associated marshland (2.2×10^6) Km² compose the essence of the marshland of southern Iraq. They are centered on the meeting of the Tigris and Euphrates Rivers in Iraq. (Bedair *et al.*, 2006).

Table 3: The Classes color key of the classified scenes.

Class	Color	Class	Color	Class	Color
Very deep water	Black	Dense plant	Dark Green	Sandy land	Orange
Deep water	Blue	Sparse plant	Light Green	Mineral land	Pink
Shallow water	Cyan	Muddy land	Brown	Dry land	Yellow

The study area covers approximately (20222.7 km²), within longitude range (45° 29' 5.07" to 46° 53' 25.60" E) and latitude range (32° 23' 1.14" to 31° 3' 18.07" N), as shown of natural color band combination in fig. 1c. The available remotely sensed data is downloaded from the website of the United States Geological Survey (USGS) Center for Earth resources, observation and science (Survery, n.d.).

Research Methodology

In order to calculate the seasonal effect of the water bodies in the Marshlands, the following methodology is adopted.

The Landsat images bands are converted from being a digital number to reflectance value that represent the true reflection of the Earth’s surface at the top of the atmosphere TOA using equation (1) (Zanter, 2016) (Chander *et al.*, 2009), which applied to the all Landsat images bands except for the thermal bands which are excluded in this study:

$$\rho\lambda = (M_p \times Q_{cal}) + A_p / \sin(\theta) \quad \dots 1$$

Where: $\rho\lambda$ =TOA planetary reflectance, M_p = reflectance multiplicative of each band, Q_{cal} = quantized calibrated pixel value (DN), A_p = reflectance additive scaling for the bands and θ = solar elevation angle. The $\rho\lambda$, M_p , Q_{cal} , A_p and θ factors values are calculated from the metadata file (MTL file) of each satellite image.

Table 4: Coverage areas of water bodies within classified Landsat images.

No.	Date	Water Body Percentage %	Water Body Area (km ²)
1.	17 January 1987	7.644	1545.7617
2.	12 July 1987	3.719	752.0364
3.	11 December 1990	4.952	1001.3904
4.	4 July 1990	3.572	722.4354
5.	23 January 1995	6.116	1236.8295
6.	18 July 1995	4.918	994.6332
7.	6 February 2000	4.329	875.4669
8.	31 July 2000	2.859	578.2662
9.	11 June 2005	2.770	560.1033
10.	24 January 2007	3.740	756.3267
11.	12 February 2014	5.684	1149.5286
12.	22 July 2014	2.871	581.0247
13.	4 February 2017	3.912	791.0649
14.	12 June 2017	3.246	656.4501

The band combination (SWIR, NIR and Green) for each satellite image is adopted to distinguish and separate the land cover features especially the water bodies.

- Applying the support vector machine SVM as a classifier to classify each image for the existed classes.
- Calculate the area and it’s percent for the water bodies in each scene for each season.
- Calculate the seasonal change for the water bodies in its area and percent.
- Analyzing the temporal variation in the water bodies classes (shallow, deep and very deep) between Winter and Summer seasons.

Results and Discussion

The rectified Landsat images bands to reflectance are classified using the support vector machine classifier where the setting that used for the classifier is illustrated in table 1. The Landsat images are classified into the following land cover features that exist in the marshland images, which are, very deep, deep and shallow water, mature, sparse and dense plant, muddy, sandy, mineral and dry land.

The classification accuracy is calculated by comparing the classifier results with the reference supervised classes for the region of interest where the classifier accuracy found to be higher than 97 percent as illustrated in table 2.

To distinguish the distribution of the all water bodies classes, fig. 2, shows the mask of the water bodies only after classification *via* SVM classifier. The classes color key is illustrated in table 3.

The overall water bodies area and percent for its different are calculated for each season as illustrated in table 4.

The differential change in the total water area and percent between the Summer and Winter seasons is calculated, see table 5, we can notice as a general behavior

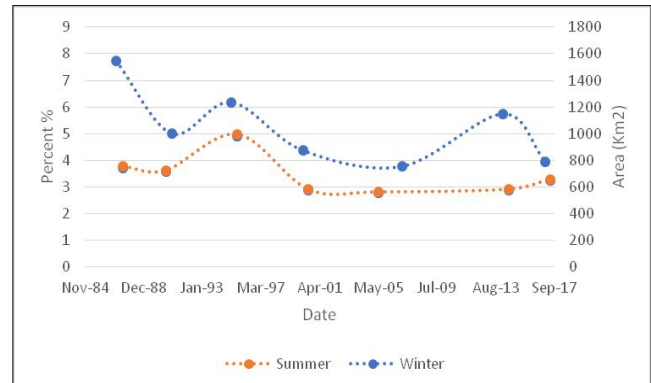


Fig. 3: Percentage area of water bodies for the two seasons.

Table 5: Percentage and area difference between the two seasons of the water bodies.

Date	Water Body Percentage %	Water Body Area (km ²)
1987	3.925	793.7253
1990	1.38	278.955
1995	1.198	242.1963
2000	1.47	297.2007
2005 & 2007	0.97	196.2234
2014	2.813	568.5039
2017	0.666	134.6148

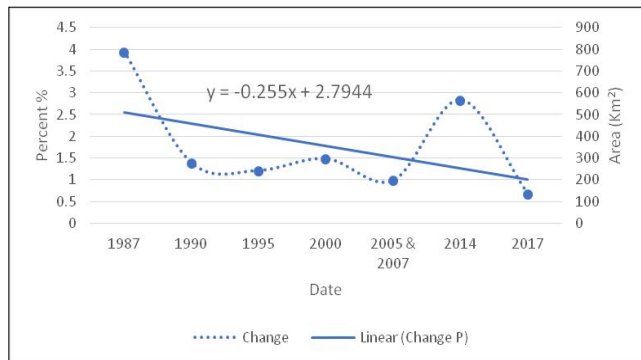


Fig. 4: The differences in the water bodies between the two seasons.

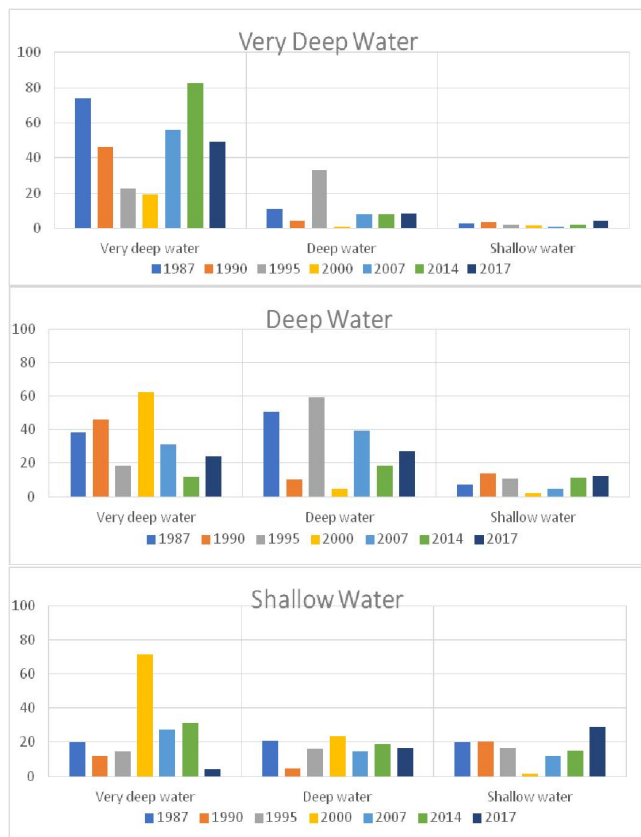


Fig. 5: Change detection for each water class between Winter and Summer season (a. very deep water, b. deep water and c. shallow water).

that all difference is degraded with time (the fitted curve) as illustrated in fig. 4. The most decreasing occurs after 1987.

The effect of the reduction in the water bodies area in the Summer season comparing with the Winter season on the water bodies classes (shallow, deep and very deep) has been analyzed by comparing each class area that registered in the Winter season with the Summer season, by calculating the percent of that class to be keep in the same class or it transforms into other class among the other scene classes (increasing or reduction in the water level), as illustrated in table 6.

In fig. 5 can be noticed that the very deep water class preserved to be in the same class with the minimal changing two other classes, (see fig. 5a), while as expected the two other classes failed to keep from transforming to other classes due to the low water level which makes the water reduction in Summer effect on them.

Conclusions

From the results obtained by studying the Iraqi Marshlands for the period 1987-2017, one can conclude the following remarks. The difference in the water bodies area between the Winter and Summer seasons is decreased especially after 1987 due to different reasons such as the reduction in water resources that supply the Iraqi Marshlands and low raining levels for the late 30 years. The shallow and deep water classes are mostly affected by the decreasing of difference in the water body between the Winter and the Summer seasons, in contrast to the very deep water which in general preserved in its class with minimal changing two other water body classes.

Acknowledgement

This research is supported by the College of Education for Pure Science Ibn-Al-Haitham, University of Baghdad.

Conflict of Interest

The author declares that there is no conflict of interests regarding the publication of this manuscript. In addition, the ethical issues, including plagiarism, informed consent, misconduct, data fabrication and/or falsification, double publication and/or submission, and redundancy have been completely observed by the authors.

Abbreviations

- Reflectance additive scaling for the bands A_{ρ}
- Digital Number of pixel DN
- Easting E

Table 6: Change detection for water classes in Winter and Summer seasons.

		Summer						
Winter	Class	1987			1990			
		Very deep water	Deep water	Shallow water	Very deep water	Deep water	Shallow water	
		Very deep water	73.663	38.553	20.034	46.413	45.771	11.987
		Deep water	10.888	50.549	20.968	4.024	10.099	4.458
		Shallow water	2.578	7.33	19.955	3.431	13.624	20.659
		Class	1995			2000		
	Very deep water		Deep water	Shallow water	Very deep water	Deep water	Shallow water	
		Very deep water	22.24	18.198	14.4	19.06	62.604	71.303
		Deep water	33.113	59.383	15.781	0.561	4.519	23.413
		Shallow water	1.968	10.728	16.692	1.779	1.878	1.731
	Class	2007			2014			
		Very deep water	Deep water	Shallow water	Very deep water	Deep water	Shallow water	
	Very deep water	55.755	31.264	27.25	82.625	11.667	31.276	
	Deep water	8.024	39.407	14.409	8.019	18.282	18.87	
	Shallow water	0.862	4.574	11.806	1.977	11.274	14.859	
	Class	2017						
		Very deep water	Deep water	Shallow water				
	Very deep water	49.325	23.908	4.124				
	Deepwater	8.471	26.915	16.634				
	Shallow water	3.872	12.126	28.98				

- Enhanced Thematic Mapper Plus (ETM+) sensor launched on-board Landsat 7 in April 1999 ETM+
- Multiple of the square meter, the SI unit of area or surface area. 1 km² is equal to: 1,000,000 square meters (m²) km²
- Metadata File of each satellite image MTL
- Moderate Resolution Imaging Spectroradiometer (MODIS) launched by NASA in 1999 MODIS
- Multispectral Scanner (MSS) sensor, launched on-board Landsat 1 in July 1972 MSS
- Reflectance multiplicative of each band M_p
- Near-I infrared NIR
- Northing N
- Operational Land Imager (OLI) sensor, launched on-board Landsat 8 in February 2018 OLI
- Picture Element Pixel
- Top of the Atmosphere planetary reflectance $\rho\lambda$
- Quantized calibrated pixel value Q_{cal}
- Short-Wave Infrared SWIR
- Support Vector Machine SVM
- Thematic Mapper (TM) sensor, launched on-board Landsat 5 in March 1984 TM
- Top of the Atmosphere TOA
- United States Geological Survey (USGS) center for Earth resources USGS
- Solar elevation angle θ

References

Albarakat, R., V. Lakshmi and C.J. Tucker (2018). Using Satellite Remote Sensing to Study the Impact of Climate and Anthropogenic Changes in the Mesopotamian Marshlands, Iraq. *MDPI, Remote Sensing.*, **10**: 1-22.

Abdul Jabbar, M.F., A.F. Al-Ma'amar and A.T. Shehab (2010). Change detections in marsh areas, south Iraq, Using remote sensing and GIS applications. *Iraqi Bulletin of Geology and Mining.*, **6(2)**: 17-39.

Abed Al-Razaq, B., S.K. Shnain and S.J. Abd Al-Hamza (2015). Monitoring of environmental variations of marshes in Iraq using Adaptive classification method. *Iraqi Journal of Science.*, **56(3B)**: 2401-2411.

AL-Ghafily, A.A. (2009). Preliminary study on the phytoplankton of marshes AL-sallal, AL-Hwizah and AL-Chebiaysh-South Iraq. *Ibn Al-Haitham Jour. for Pure and Appl. Sci.*, **22(1)**: pp. 19-32.

Anon., n.d. *Scientific and Cultural Organization*, <http://whc.unesco.org/en/list>: UNESCO, United Nations Educational.

Bedair, H.M., H.T. Al Saadb and N.A. Salman (2006). Iraq's Southern Marshes Something Special To Be. *Marsh Bulletin.*, **2(1)**: 99-126.

Chander, G., B.L. Markham and D.L. Helder (2009). Summary of current radiometric calibration coefficients for Landsat MSS, TM, ETM+ and EO-1 ALI sensors. *Remote Sensing of Environment.*, **113(5)**: 893-903.

Fitzpatrick, R.W. (2004). *Changes in soil and water characteristics of natural, drained and re-flooded soils in the Mesopotamian marshlands: Implications for land*

- management planning*, South Australia: CSIRO Land and Water.
- Jaquet, J.M., S. Schwarzer and K. Allenbach (2005). *Iraqi Marshlands Observation System*, Kenya: UNEP.
- Ma, Y. and G. Guo (2014). *Support Vector Machines Applications*. Switzerland: Springer.
- Muhsin, I.J. (2011). Al-hawizeh marsh monitoring method using remotely Sensed images. *Iraqi Journal of Science*, **52(3)**: 381-387.
- Muhsin, I.J. and M.J. Kadhim (2017). Monitoring of south Iraq marshes using classification and change detection techniques. *Iraqi Journal of Physics.*, **15(33)**: 78-86.
- Naji, T.A. and A.J. Hatem (2013). New Adaptive Satellite Image Classification Technique for Al habbinya Region West of Iraq. *bn Al-Haitham Jour. for Pure & Appl. Sci.*, **26(2)**: 143-149.
- Saleh, S.A.H. (2012). Temporal Change Detection of AL- Hammar Marsh-IRAQ Using. *Global Journal of HUMAN SOCIAL SCIENCE Geography & Environmental geosciences.*, **12(12)**: 1-8.
- Saleh, S.A.H. and E.H. Nasser (2014). *Analysis of environmental changes in Iraq Marshes by Remote Sensing*. Germany: LAP Lambert Academic Publishing.
- Salman, H.M. (2019). Text Classification Based on Weighted Extreme Learning Machine. *Ibn Al-Haitham Jour. for Pure & Appl. Sci.*, **32(1)**: 198-205.
- Survery, U.S.G., n.d. *Earth Explorer-Home*. (Online Available at: <https://earthexplorer.usgs.gov/>).
- Suykens, J.A.K. M. Signoretto and A. Argyriou (2015). *Regularization, Optimization, Kernels and Support Vector Machines*. New York: Taylor & Francis.
- Zanter, K. (2016). *Landsat 8 (L8) data user handbook*, South Dakota: USGS.